HHS Public Access

Author manuscript

Transplantation. Author manuscript; available in PMC 2016 August 01.

Published in final edited form as:

Transplantation. 2015 August ; 99(8): 1574–1581. doi:10.1097/TP.0000000000000682.

Monitoring of allogeneic islet grafts in nonhuman primates using magnetic resonance imaging

Ping Wang[1,*], **Christian Schuetz**[2,3,*], **Prashanth Vallabhajosyula**[4,*,◆], **Zdravka Medarova**[1], **Aseda Tena**[4], **Lingling Wei**[4,#], **Kazuhiko Yamada**[4], **Shaoping Deng**[2], **James F. Markmann**[2], **David H. Sachs**[4], and **Anna Moore**[1]

[1]Molecular Imaging Laboratory, MGH/MIT/HMS Athinoula A. Martinos Center for Biomedical Imaging, Department of Radiology, Massachusetts General Hospital, Harvard Medical School, Charlestown, Massachusetts 02129, USA

[2]Division of Transplantation, Department of Surgery, Massachusetts General Hospital, Harvard Medical School, Boston, MA, USA

[3]Department of Stem Cell and Regenerative Biology, Harvard Stem Cell Institute, Harvard University, Cambridge, MA, USA

[4]Transplantation Biology Research Center, Massachusetts General Hospital, Harvard Medical School, Charlestown, MA, USA

Abstract

Background—Information regarding the longevity of transplanted pancreatic islet grafts could provide valuable information for treatment options. In our previous studies we showed that isolated autologous pancreatic islets could be labeled with iron oxide nanoparticles and monitored following transplantation using magnetic resonance imaging. Here, we report on in vivo monitoring of a secondary damage that occurs at the later stages due to allogeneic immune rejection.

Methods—In the proof-o-principle studies, iron oxide-labeled autologous pancreatic islets were transplanted under the renal capsules of non-human primates. To demonstrate acute graft loss, the animals were injected with streptozotocin (STZ). Graft monitoring was performed by in vivo MRI.

Address correspondence to: Anna Moore, Ph.D., Molecular Imaging Laboratory, MGH/MIT/HMS Athinoula A. Martinos Center for Biomedical Imaging, Massachusetts General Hospital/ Harvard Medical School, Building 75, 13th Street, Charlestown, MA 02129., amoore@helix.mgh.harvard.edu.

◆(Prashanth Vallabhajosyula) - present address: Division of Cardiovascular Surgery, University of Pennsylvania Health System

#(Lingling Wei) - present address: Center for Cell Transplantation, Institute of Organ Transplantation, Sichuan Academy of Medical Sciences & Sichuan Provincial People's Hospital, Chendu, China.

*these authors contributed equally to the study

Authors declare no potential conflicts of interest relevant to this publication.

Author Contributions: P.W. performed the MRI scanning, image analysis, histology staining and participated in writing the manuscript; C.S. performed autologous transplantation, histology, lab works and participated in writing the manuscript; P.V. performed allogeneic transplantation, lab works and participated in writing the manuscript; Z.M. performed MRI and image analysis and participated in writing the manuscript; A.T. and L.W. assisted with animal handling during surgery and MR imaging; S.D. assisted with islet isolation and in vitro testing; K.Y and J.M. directed the surgery, participated in data analysis and drafting the manuscript; D.S. discussed the aims of the project, participated in data analysis and drafting the manuscript, A.M. conceived the idea of the project and wrote the manuscript. A.M. is the guarantor of this work and, as such, has full access to all the data in the study and takes responsibility for the integrity of the data and the accuracy of the data analysis.

Next, iron oxide-labeled allogeneic islets were transplanted into the liver and monitored by MRI after withdrawal of immunosuppression.

Results—In autologous model we observed a pronounced drop in graft volume after STZ challenge as assessed by MRI. In allogeneic model of islet transplantation, there was an initial islet loss after the procedure followed by relative stabilization of the graft volume. After immunosuppression was discontinued there was a noticeable drop in graft volume that gradually continued during the course of the study. Importantly, the loss of graft volume observed on MR preceded the raise in blood glucose.

Conclusion—This study demonstrated that in vivo MRI was able to reveal graft volume loss prior to any changes in blood glucose that can be measured by standard methods. We believe that these results could provide means for clinicians to follow islet fate non-invasively and longitudinally using clinically relevant scanners.

Introduction

Islet transplantation has evolved as the most promising treatment modality for type 1 diabetes (T1D) (1). In spite of the success of the Edmonton protocol, the outcome of islet transplantation remains suboptimal. According to the most recent report from the Collaborative Islet Transplant Registry, insulin independence at 3 years after transplant is achieved at 44% in the most recent era (2007–2010; (2)). The factors contributing to the graft loss include instant blood-mediated inflammatory reaction (IBMIR) (3; 4), ischemia induced islet apoptosis (5), toxicity of immunosuppressants (6), recurrence of autoimmunity (7; 8), and most importantly allogeneic immune rejection (9). Monitoring of the above-mentioned damages in islet grafts is a prerequisite for a clinical graft salvage intervention. The currently available monitoring parameters for assessing islet graft viability and function, such as blood glucose level, serum C-peptide level and glucose tolerance test are considered relatively late markers of islet graft dysfunction. Biopsy is a method that can provide direct evidence of islet damage but contrary to solid organ transplantation this invasive approach could not be widely applied due to the small size of islet grafts and their relatively low frequency after dispersion in a large organ such as the liver (10).

The inability to directly monitor islet grafts over time severely limits our understanding of mechanisms regarding declining graft function. Magnetic resonance imaging (MRI) of islet grafts labeled with magnetic dextran-coated iron oxide nanoparticles could provide the necessary information. Our group and other investigators (11–14) have developed an approach for detection and monitoring of transplanted labeled islets non-invasively using MRI. Studies from our group and others have also demonstrated the ability of MRI to detect islet loss in small animal models at the early stages after transplantation (15–18). While first clinical trials performed in Europe showed no correlation between the number of injected islets and the number of hypointense spots (19) the subsequent study revealed a 60% decrease in graft volume one week after transplantation in eight patients (20). Our study in non-human primates (21) for the first time demonstrated the capability of an MR imaging approach for monitoring autologous grafts longitudinally. However, it still remains unclear whether sequential MRI monitoring could be applied for detection of islet loss that occurs at later stages due to allogeneic immune rejection. In this study we have assessed the

applicability of longitudinal in vivo MRI for monitoring of immune rejection in allogeneic grafts after withdrawal of immune suppression in diabetic non-human primates, using clinical scanners. We demonstrate that MR imaging is capable of detecting islet loss prior to any changes in blood glucose measured by standard methods. We believe that the results of this study could provide an opportunity to monitor the selection of an appropriate treatment to rescue islet grafts from immune damage before they are lost to rejection.

MATERIALS AND METHODS

Animal care and diabetes induction

All animal experiments were performed in compliance with institutional guidelines and were approved by the Institutional Animal Care and Use Committee at the Massachusetts General Hospital. Donor and recipient baboons (Papio hamadryas, Manheimer Foundation, Homestead, FL, USA) were housed in an animal facility at MGH and quarantined for 6 weeks before study. Baboons (n=2; male, 8–10kg/3–4yrs old, B255, B267) were used for autologous renal transplantation. Baboons (n=2; male, 8–10kg/3–4yrs old, B180, B183) were used as recipients for allogeneic islets transplanted in the liver. For diabetes induction these animals were injected intravenously with streptozotocin (STZ) (Sigma, St. Louis, MO; 100 mg/kg). Animals were considered diabetic when fasting blood glucose levels were >300 mg/dl on three consecutive days. These two diabetic baboons were then treated with injections of insulin guided by fasting blood glucose (FBG) measurements. The following tests were performed weekly upon peripheral blood: a complete blood count (CBC), electrolytes, renal profile, liver profile, lipid metabolism. Serum C-peptide levels were measured by radioimmunoassay (Human C-peptide RIA Kit, Linco Research, Inc., St. Charles, MO).

Autologous and allogeneic islet transplantation, graft function assessment and immunosuppression treatment regimens

Protocols for islet harvest and mixed lymphocyte reaction are described online in Supplemental Digital Content.

For all pre-transplantation islet labeling, we used the FDA approved dextran-coated iron oxide nanoparticles Feridex (ferumoxides, Advanced Magnetics, Cambridge, MA). Isolated islets were incubated with Feridex at concentration of 400μg iron/ml in CMRL 1066 Culture media. After overnight culture, the labeled islets were washed three times in Hanks Balanced Salt Solution and used for islet transplantation.

For autologous transplantation the islets (10,000–82,000 IEQ) were injected underneath the renal capsule. To investigate whether secondary islet graft loss could be detected by MRI, we used an acute model by injecting these animals with high dose of STZ (100 mg/kg; B255 on day 83 and B267 on day 201 post islet transplantation; timeline is shown in Fig. 1A).

For allogeneic intrahepatic transplantation approximately 100,000 IEQ islets were infused into the recipients (B180 and B183).

Graft function was assessed through fasting blood glucose (FBG), hemoglobin A1C, C-peptide levels and intravenous glucose tolerance testing (IVGTT).

The immunosuppressive protocols for allogeneic transplantation include Rapamycin IM daily to achieve target blood levels between 20–30 ng/ml; Tacrolimus IM daily (Trough 4–10 ng/ml); Daclizumab IV every 14 days for a total of five doses. The immunosuppressive treatment was initiated on the day of transplantation. Whole-blood drug levels were determined by microparticle enzyme immunoassay. The immunosuppressive therapy was completely withdrawn early (day 49) and late (day 104) during the graft establishment for B183 and B180, respectively. Insulin was not administered unless fasting blood glucose levels were consistently (two blood glucose readings) above 300 mg/dl. The date of graft failure was defined as the first of 3 consecutive days of fasting blood glucose levels >300 mg/dl unless the blood glucose subsequently normalized without insulin therapy. The time line of the experiments for these two animals is summarized in Fig. 1B.

Longitudinal magnetic resonance imaging

Before MRI the baboons were fasted for 8 hours. Then the animals were sedated with Ketamine i.m. (10mg/kg) and maintained on intravenous propofol sedation. Endotracheal intubation was performed to secure the airway and the animal was transported to the MRI unit and placed supine on the MRI table. The vital signs of the animals were continuously monitored during the MRI. The MR images were acquired using a 1.5 T Siemens Trio magnet equipped with 6-channel body matrix coil and spine-array coil (Siemens Healthcare, Germany). Imaging parameters and image analysis are described online in Supplemental Digital Content.

Islet transplant biopsy and histological evaluation

Surgical biopsies were performed at different time points via a laparotomy. Tissues were fixed in 10% formalin, embedded in paraffin and sectioned at 4μm sections. To visualize labeled islet grafts in the liver using fluorescence microscopy, tissues sections were incubated with mouse monoclonal antibody to dextran (1:100 dilution; Stemcell Technologies, Vancouver, BC, Canada) and with rabbit anti-human polyclonal antibody to insulin (1:100 dilution, Santa Cruz Biotechnology, Santa Cruz, CA), followed by an Alexa Fluor 594 conjugated secondary goat anti-mouse IgG (1:100 dilution, Invitrogen, Eugene, OR) and DyLight 488-labeled goat anti-rabbit IgG secondary antibody (1:100 dilution, Abcam, Cambridge, MA). To examine the infiltration of immune cells in islet grafts, the sections were also incubated with mouse anti-human CD3 antibody (1:100 dilution, Dako North America, Inc., Carpinteria, CA) and with rabbit anti-human polyclonal antibody to insulin, followed by incubation of secondary antibody as described above. After incubation, slides were mounted with a mounting medium containing DAPI (Vectashield, Vector Laboratories, Inc., Burlingame, CA). Images were acquired using a Nikon Eclipse 50i microscope using a SPOT 7.4 Slider RTKE CCD camera (Diagnostic Instruments, Sterling Heights, MI) and analyzed with iVision 4.015 software.

RESULTS

Proof-of-principle studies in autologous grafts

As a proof-of-principle we first determined whether we could monitor the loss of established islet grafts in an autologous model of renal transplantation in baboons. The animals received islet transplants under the kidney capsule and were monitored by MR imaging as we described previously (21). To investigate whether MR imaging is capable of detecting acute graft loss, the animals were injected with streptozotocin (STZ) after initial graft loss was complete and the grafts were established (timeline is shown in Fig. 1A). As expected, following the STZ injection, the animals became hyperglycemic with FBG > 500 mg/dl and higher. Within 7–10 days after injection we observed a pronounced drop (50% of pre-STZ levels) in graft volume as assessed by MRI (Fig. 2). Intravenous glucose tolerance test (IVGTT) confirmed our imaging data demonstrating impaired glucose tolerance after STZ injection (Supplemental Fig. 1A). Similarly, biopsy of the grafts showed insulin positive cells under the kidney capsule post islet transplant, which were not found after SZT injection as indicated by the staining of the necropsy tissue sections (Supplemental Fig. 1B). The results of these studies served in lieu of a “positive control” and indicated that in vivo imaging could detect changes in graft volume caused by islet destruction by acute action of STZ.

Feridex-labeled islets successfully restored normoglycemia after allogeneic transplantation

We next asked a question whether in vivo MRI could detect changes in the volumes of established grafts caused by immune rejection. To imitate the potential clinical scenario we first showed that the Feridex-labeled transplanted grafts were capable of restoring normoglycemia in animals rendered diabetic by STZ injection (timeline is shown in Fig. 1B). The elevated blood glucose levels and decreased C-peptide levels after STZ treatment were observed in these two animals (Fig. 3A, B). Both animals needed insulin injections before islet transplantation, which indicated that the remaining islets in the pancreas were not functioning properly. The FBG levels of the recipients were normalized (< 150mg/dl) within 3 days after allogeneic islet transplantation. Until the immunosuppressive therapies were discontinued, the following tests were normal (Fig. 3A–C): 1) animals maintained normoglycemia; 2) HbA1c levels were maintained at approximately 4.1% (21 mmol/mol); 3) positive basal C peptide levels were > 2ng/ml; 4) normal IVGTT function was displayed throughout the course of immunosuppressive therapies. The results of these studies supported our previous observations (21) that labeling did not affect islet function after transplantation.

In vivo MR imaging of labeled allogeneic grafts

To monitor transplanted labeled grafts we performed longitudinal in vivo MR imaging starting on the next day after the procedure. On the T2* weighted MR images, the pre-transplant liver parenchyma was characterized by considerable homogeneity (Supplemental Fig. 2). By contrast, islets transplanted intrahepatically appeared as distinct voids of signal loss dispersed throughout the liver (Fig. 4A). As expected, there was an initial sharp islet loss two to three weeks post transplantation followed by relative stabilization of the graft

volume in B180 and continues volume decline in B183 (Fig. 4B, C). During this time animals were maintained on immunosuppression as described in Materials and Methods. After immunosuppression was discontinued there was a noticeable drop in graft volume. This drop gradually continued during the course of the experiments and at the time of euthanasia accounted for 5–10% of initial graft volume (Fig. 4B, C). Importantly, the drop in graft volume was significant regardless of whether immunosuppression was discontinued early (B183, Fig. 4B) or late during graft establishment (Fig. 4C). In both cases the loss of graft volume observed on MR preceded the raise in blood glucose, which was evident 30 and 36 days post immunosuppression withdrawal in respective animals (Fig. 4B, C). Animals exhibited impaired glucose tolerance (Fig. 3C) and insulin therapy was eventually initiated (Fig. 4B, C; plus symbol). These results indicate that in vivo MR imaging was able to detect changes in graft volume indicative of islet loss prior to any detectable changes in blood glucose.

Histological analysis of islet grafts

Histological analysis of liver biopsy performed prior to withdrawal of immune suppression showed the presence of the labeled graft distributed throughout the liver (Fig. 5A). Insulin staining revealed that the grafts were functioning at this time, which was confirmed by normal blood glucose levels. Co-staining for insulin and dextran on the nanoparticles showed that the latter were present in the cytoplasm of islet graft cells (Fig. 5A) Earlier studies, both from our laboratory and others, showed that while these nanoparticles are generally biodegradable, they are capable of remaining intact inside islet cells for considerable lengths of time (11–12, 14, 16, 18). Before withdrawal of immunosuppression, islet grafts stained positive for insulin and appeared morphologically intact as evident from Fig. 5A. Following withdrawal of immunosuppression insulin staining was mostly lost in these islet grafts, which coincided with increased infiltration of CD3-positive T cells (Fig. 5B, day 62), which eventually disappeared following the destruction of the graft (Fig. 5B, day 109). However, residual insulin staining was detectable in infiltrated grafts (Fig. 5C). This coincided with residual anti-dextran staining showing compartmentalized nanoparticles (Fig. 5D, arrow), which was evidently sufficient for generating MR signal. It has previously been demonstrated that nanoparticles released from dying islets diffuse throughout the tissue at concentrations that are too low for MRI detection (16). The histological analysis of intra-hepatic islet grafts confirms the progressive rejection of allogeneic islets upon withdrawal of immunosuppression, and attests to the physical destruction of islets correlating to the loss of islet signal on MRI.

DISCUSSION

Success of islet transplantation in restoring normoglycemia depends on multiple factors including immune rejection, which necessitates the use of immunosuppressive therapies that are known to be toxic to transplanted grafts contributing to their progressive dysfunction (6; 22). As emphasized on http://diabetes.niddk.nih.gov/dm/pubs/pancreaticislet/ and as extensive experience in solid organ transplantation has shown immunosuppressive medications have significant short and long-term side effects, and their long-term effects are still not fully known. Most importantly, immunosuppressive medications also increase the

risk of developing certain cancers. Modulation of immunosuppressive therapies with the aim of reducing their side effects and ultimately achieving immune tolerance are the major goals in islet transplant research. In order to reduce or eliminate immunosuppressants, clinicians need a tool that would allow them to monitor the status of transplanted islets over time. In vivo imaging approach has recently emerged as a novel method to monitor the fate of islets directly in a clinical setting (23). In vivo magnetic resonance imaging utilizing labeled islets has already demonstrated its utility for monitoring transplanted grafts in small (11–18; 24–26) and large (21; 27) animals. Two clinical trials showed some promise for monitoring islet grafts during initial post-transplant follow-up period (19; 20). We believe that this MRI approach could be further used for detecting changes in the established islet grafts during the course immunosuppressive therapy or as a follow up to any other intervention that might be essential for islet graft survival.

Therefore, in our current study we set the goal to demonstrate that MR imaging could be used for detecting failure of established grafts longitudinally in large animals. In our proof-of-principle studies we demonstrated that acute loss of established grafts caused by STZ injection in autologous transplants could be readily detected by MR imaging. Severe loss of islet grafts observed by MRI was accompanied by a rise in blood glucose within 48 hours. Next, we set out to demonstrate that this in vivo imaging method would be applicable to the situation similar to that observed in clinic when islet allograft loss is caused by immune rejection. To confirm that labeled grafts were functional we transplanted them in diabetic animals and observed normalization of their blood glucose that occurred approximately three days post transplant. We next challenged these islet grafts by withdrawal of immune suppression at early or late period of the graft establishment. This discontinuation of immune suppression caused gradual loss of islet grafts in both cases as detected by MRI and confirmed by histology. Importantly, we found that the drop in islet graft volume occurred prior to the changes in blood glucose detected by conventional methods. Interestingly, similar results have been previously demonstrated in mice using bioluminescence imaging, a non-clinical imaging modality (28). The finding that normoglycemia was maintained is in line with the clinical finding in T1D patients, that a small remaining beta cell mass can maintain normoglycemia until a certain threshold is reached (29). In our study abnormal FBG readings were observed at 15% (B183) and 37% (B180) of the initial signal remained. It is also possible that since allo-immune rejection-induced islet destruction was gradual there was a gradual release of insulin from dying islets that maintained “virtual” normoglycemia in spite of the fact that islet volume was already decreased. We believe that this observation is of high significance for the following reasons. First, because islet damage is not obvious from the blood glucose readings during gradual destruction until a critical beta cell mass threshold is reached, it could create a false sense of security regarding graft stability and function. This could lead to underestimations/delay in prescribing therapeutic interventions. Second, the ability to detect islet damage early in the process could provide valuable information for clinicians about the dose and timing of immunosuppressive therapy. It would allow for monitoring the effectiveness of this and other therapeutic interventions and can be exploited to inform immunosuppressive therapy, similar to graft biopsies in solid organ transplantation. It can even create the “windows” when the dose of toxic immunosuppressants could be significantly reduced but then could be increased

immediately if any loss in the graft is detected. Third, in addition to immune rejection autoimmunity may be another reason responsible for the fact that only 20% of patients remain insulin independent 3 years after islet transplantation in spite of the success of the Edmonton protocol (30). Imaging would allow the correlation between islet mass and markers of autoimmunity such as beta-cell-specific antibodies and/or effector T cells.

Another important observation made in our study deals with heterogeneity of the time course and the pattern of the graft rejection in non-human primates that was not observed in small rodents. This heterogeneity in imaging pattern was clearly demonstrated in clinical trials where patients exhibited various numbers of dark voids in their livers largely independent of the number of the islets infused (19). This points to the necessity of testing novel research tools in large animals bringing experimental conditions as close as possible to potential clinical scenario and providing the basis for individualized monitoring protocols that catalyzes personalized medicine.

Finally, this approach could be instrumental for developing novel cell replacement therapies in diabetes. Recent seminal study by Kroon et al. (31) and Rezania et al. (32) demonstrated successful application of human embryonic stem cell (hESC)-derived pancreatic progenitors for restoring normoglycemia (31). First phase clinical trials using this approach are currently underway. Protocols describing generation of insulin-producing beta-cells by differentiation of human pluripotent stem cells (hPSCs) along the pancreatic lineage have been developed and are now widely available for diabetes researches (33). Regardless of the source of beta cells available for transplantation and the cause of their death there is a need to detect and monitor these grafts over time in experimental animals and in humans. The approach described above could assist researches in determining whether the grafts generated from these new cell sources are viable and functional.

Supplementary Material

Refer to Web version on PubMed Central for supplementary material.

Acknowledgments

Support:

Ping Wang, Zdravka Medarova, Anna Moore - R01DK078615

Aseda Tena - 5U19AI102405-02 and U01AI074634

Prashanth Vallabhajosyula - U01AI074634

David Sachs, Kazuhiko Yamada - 5R01AI086134-05, 5U19AI102405-02, U01AI074634

Lingling Wei - China Scholarship Council (CSC)

Christian Schuetz, Shaoping Deng, James F. Markmann – MGH institutional support

Authors want to thank Dr. Zurab Machaidze for help with animal handling during surgery, post-surgery care and MR imaging. This work was supported in part by R01DK078615 from NIH/NIDDK to A.M.

Abbreviations

CBC	complete blood count
FBG	fasting blood glucose (FBG)
IBMIR	instant blood-mediated inflammatory reaction
IVGTT	Intravenous glucose tolerance test
MRI	magnetic resonance imaging
STZ	streptozotocin

References

1. McCall M, Shapiro AM. Update on islet transplantation. Cold Spring Harb Perspect Med. 2012; 2:a007823. [PubMed: 22762022]
2. Barton FB, Rickels MR, Alejandro R, et al. Improvement in outcomes of clinical islet transplantation: 1999–2010. Diab Care. 2012; 35:1436.
3. Bennet W, Groth CG, Larsson R, Nilsson B, Korsgren O. Isolated human islets trigger an instant blood mediated inflammatory reaction: implications for intraportal islet transplantation as a treatment for patients with type 1 diabetes. Ups J Med Sci. 2000; 105:125. [PubMed: 11095109]
4. Moberg L, Johansson H, Lukinius A, et al. Production of tissue factor by pancreatic islet cells as a trigger of detrimental thrombotic reactions in clinical islet transplantation. Lancet. 2002; 360:2039. [PubMed: 12504401]
5. Stadlbauer V, Schaffellner S, Iberer F, et al. Occurance of apoptosis during ischemia in porcine pancreas islet cells. Int J Artif Organs. 2003; 26:205. [PubMed: 12703886]
6. Niclauss N, Bosco D, Morel P, Giovannoni L, Berney T, Parnaud G. Rapamycin impairs proliferation of transplanted islet beta cells. Transplantation. 2011; 91:714. [PubMed: 21297554]
7. Burke GW 3rd, Vendrame F, Pileggi A, Ciancio G, Reijonen H, Pugliese A. Recurrence of autoimmunity following pancreas transplantation. Curr Diab Rep. 2011; 11:413. [PubMed: 21660419]
8. Huurman VA, Hilbrands R, Pinkse GG, et al. Cellular islet autoimmunity associates with clinical outcome of islet cell transplantation. PloS One. 2008; 3:e2435. [PubMed: 18560516]
9. Huurman VA, van der Torren CR, Gillard P, et al. Immune responses against islet allografts during tapering of immunosuppression--a pilot study in 5 subjects. Clin Exp Immunol. 2012; 169:190. [PubMed: 22774994]
10. Toso C, Isse K, Demetris AJ, et al. Histologic graft assessment after clinical islet transplantation. Transplantation. 2009; 88:1286. [PubMed: 19996928]
11. Evgenov NV, Medarova Z, Dai G, Bonner-Weir S, Moore A. In vivo imaging of islet transplantation. Nat Med. 2006; 12:144. [PubMed: 16380717]
12. Medarova Z, Evgenov NV, Dai G, Bonner-Weir S, Moore A. In vivo multimodal imaging of transplanted pancreatic islets. Nature Protoc. 2006; 1:429. [PubMed: 17406265]
13. Jirak D, Kriz J, Herynek V, et al. MRI of transplanted pancreatic islets. Magn Reson Med. 2004; 52:1228. [PubMed: 15562474]
14. Tai JH, Foster P, Rosales A, et al. Imaging islets labeled with magnetic nanoparticles at 1. 5 Tesla. Diabetes. 2006; 55:2931. [PubMed: 17065328]
15. Kriz J, Jirak D, Girman P, et al. Magnetic resonance imaging of pancreatic islets in tolerance and rejection. Transplantation. 2005; 80:1596. [PubMed: 16371931]
16. Evgenov NV, Medarova Z, Pratt J, et al. In vivo imaging of immune rejection in transplanted pancreatic islets. Diabetes. 2006; 55:2419. [PubMed: 16936189]
17. Kriz J, Jirak D, Berkova Z, et al. Detection of pancreatic islet allograft impairment in advance of functional failure using magnetic resonance imaging. Transpl Int. 2012; 25:250. [PubMed: 22188036]

18. Borot S, Crowe LA, Parnaud G, et al. Quantification of islet loss and graft functionality during immune rejection by 3-tesla MRI in a rat model. Transplantation. 2013; 96:438. [PubMed: 23902991]
19. Toso C, Vallee JP, Morel P, et al. Clinical magnetic resonance imaging of pancreatic islet grafts after iron nanoparticle labeling. Am J Transplant. 2008; 8:701. [PubMed: 18294167]
20. Saudek F, Jirak D, Girman P, et al. Magnetic resonance imaging of pancreatic islets transplanted into the liver in humans. Transplantation. 2010; 90:1602. [PubMed: 21197715]
21. Medarova Z, Vallabhajosyula P, Tena A, et al. In vivo imaging of autologous islet grafts in the liver and under the kidney capsule in non-human primates. Transplantation. 2009; 87:1659. [PubMed: 19502957]
22. Zahr E, Molano RD, Pileggi A, et al. Rapamycin impairs in vivo proliferation of islet beta-cells. Transplantation. 2007; 84:1576. [PubMed: 18165767]
23. Wang P, Medarova Z, Moore A. Molecular imaging: a promising tool to monitor islet transplantation. J Transplant. 2011; 2011:202915. [PubMed: 22013504]
24. Barnett BP, Kraitchman DL, Lauzon C, et al. Radiopaque alginate microcapsules for X-ray visualization and immunoprotection of cellular therapeutics. Mol Pharm. 2006; 3:531. [PubMed: 17009852]
25. Barnett BP, Ruiz-Cabello J, Hota P, et al. Fluorocapsules for improved function, immunoprotection, and visualization of cellular therapeutics with MR, US, and CT imaging. Radiology. 2011; 258:182. [PubMed: 20971778]
26. Barnett BP, Ruiz-Cabello J, Hota P, et al. Use of perfluorocarbon nanoparticles for non-invasive multimodal cell tracking of human pancreatic islets. Contrast Media Mol Imaging. 2011; 6:251. [PubMed: 21861285]
27. Barnett BP, Arepally A, Karmarkar PV, et al. Magnetic resonance-guided, real-time targeted delivery and imaging of magnetocapsules immunoprotecting pancreatic islet cells. Nat Med. 2007; 13:986. [PubMed: 17660829]
28. Chen X, Zhang X, Larson CS, Baker MS, Kaufman DB. In vivo bioluminescence imaging of transplanted islets and early detection of graft rejection. Transplantation. 2006; 81:1421. [PubMed: 16732180]
29. Eisenbarth GS. Type I diabetes mellitus. A chronic autoimmune disease. N Engl J Med. 1986; 314:1360. [PubMed: 3517648]
30. Alejandro R, Barton FB, Hering BJ, Wease S. Collaborative Islet Transplant Registry I: 2008 Update from the Collaborative Islet Transplant Registry. Transplantation. 2008; 86:1783. [PubMed: 19104422]
31. Kroon E, Martinson LA, Kadoya K, et al. Pancreatic endoderm derived from human embryonic stem cells generates glucose-responsive insulin-secreting cells in vivo. Nat Biotechnol. 2008; 26:443. [PubMed: 18288110]
32. Rezania A, Bruin JE, Riedel MJ, et al. Maturation of human embryonic stem cell-derived pancreatic progenitors into functional islets capable of treating pre-existing diabetes in mice. Diabetes. 2012; 61:2016. [PubMed: 22740171]
33. Van Hoof D, Liku ME. Directed differentiation of human pluripotent stem cells along the pancreatic endocrine lineage. Meth Mol Biol. 2013; 997:127.

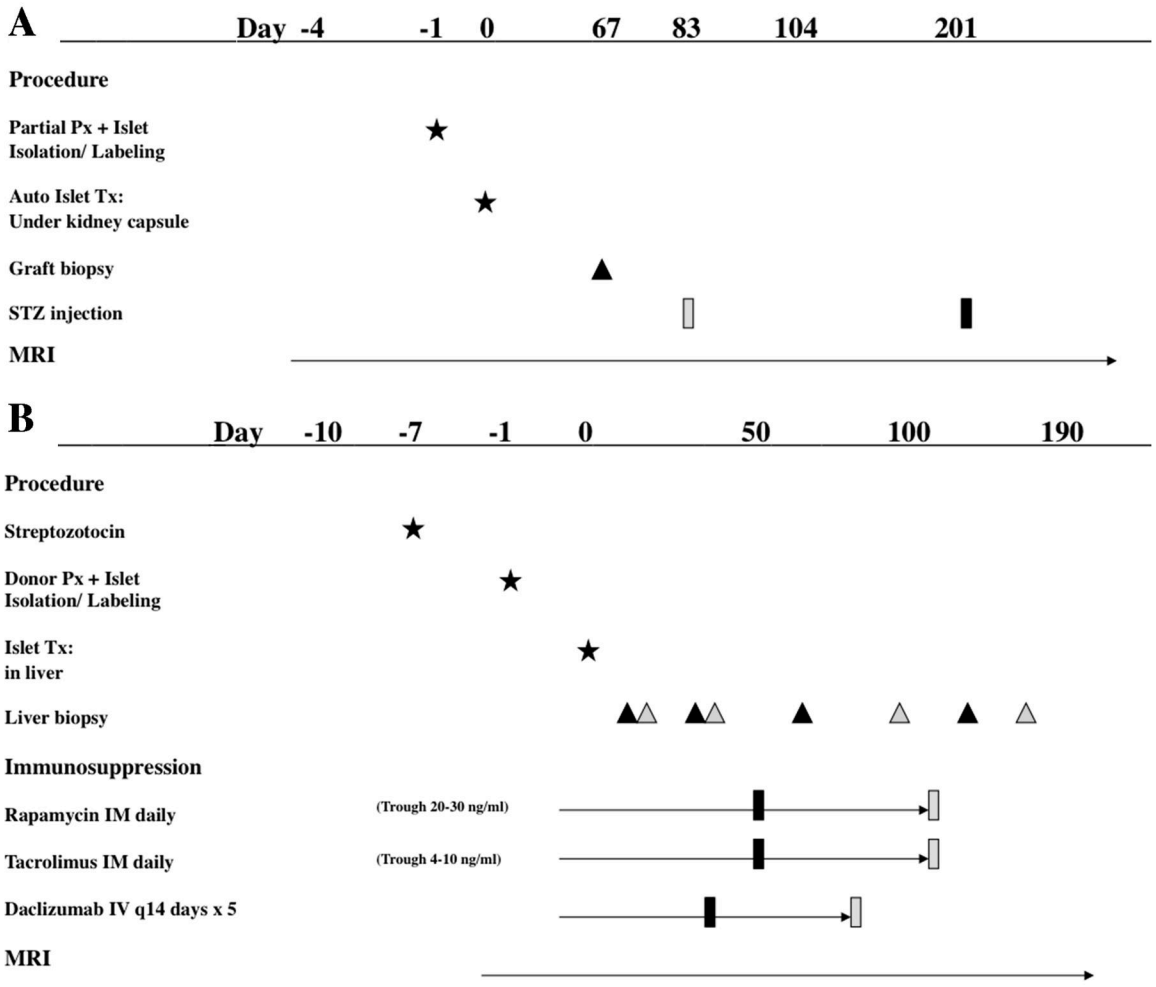

Figure 1.

Timelines for islet transplantation experiments. A: Timeline for autologous islet transplantation under the kidney capsule. Two baboons (B255, grey; B267, black) received partial Px one day prior to islet transplantation. Autologous islets labeled with iron oxide nanoparticles were then transplanted under the kidney capsule and monitored by MRI. B: Timeline for allogeneic islet transplantation in the liver. Two baboons (B180, grey; B183, black) were rendered diabetic with STZ injections seven days prior to islet transplantation. Allogeneic islets labeled with iron oxide nanoparticles were transplanted intrahepatically and monitored by MRI. Immunosuppression was administered as shown.

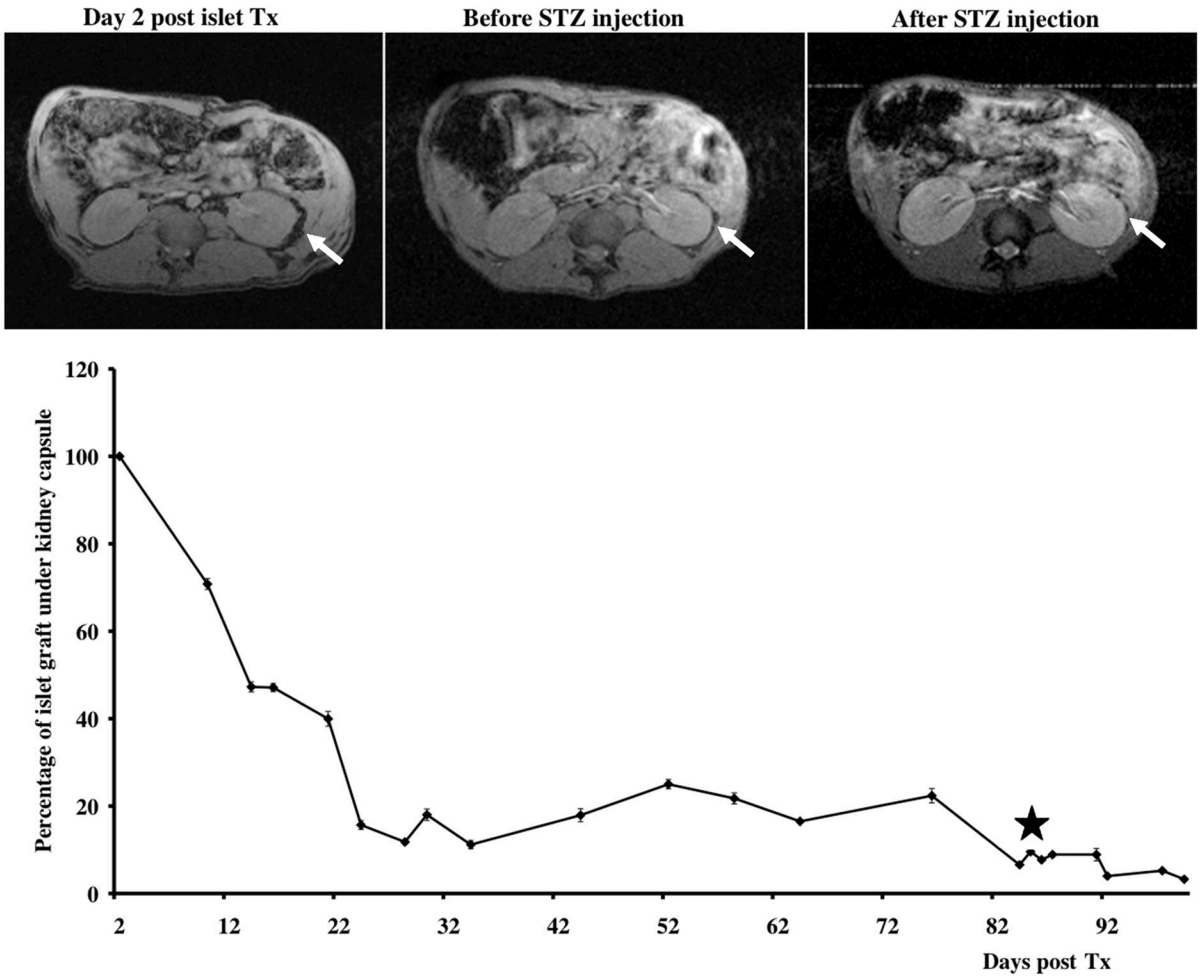

Figure 2.

Longitudinal MR imaging of autologous grafts. Top: Representative MR images of the autologous transplantation time course (arrows – transplant under the kidney capsule). Bottom: Semiquantitative assessment of graft longevity demonstrates notable drop in graft volume followed by STZ administration (star).

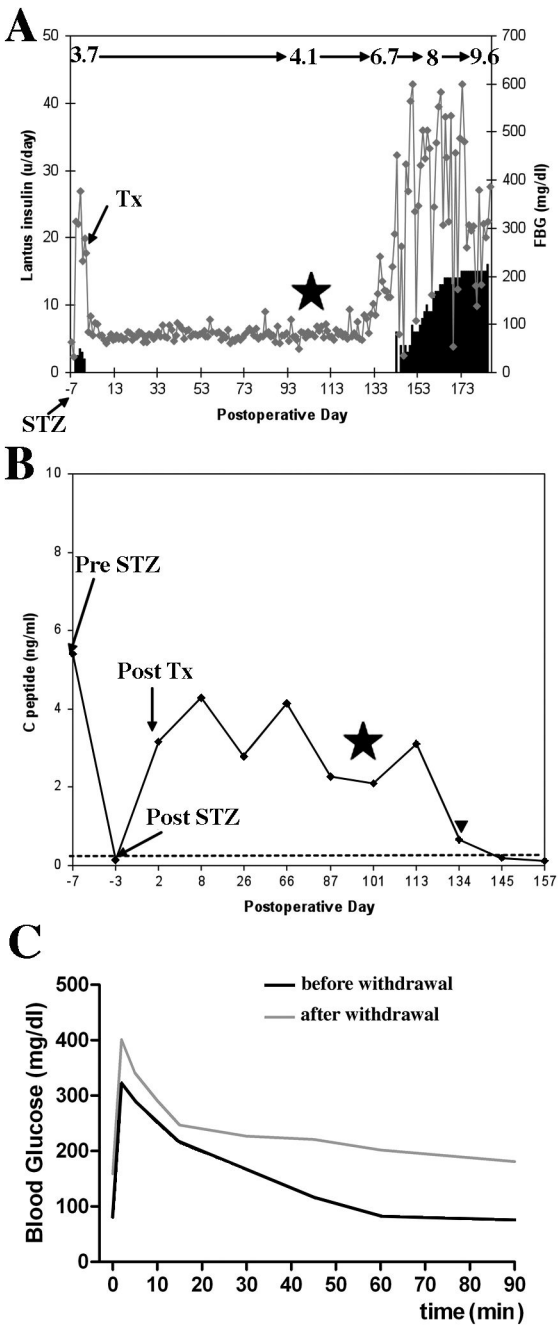

Figure 3.

Recipients of allogeneic islets maintain normal fasting glucose regulation post-islet transplant (data for B180 are shown). A: FBG and hemoglobin A1C values (denoted on top of the graph) during the course of the study. B: C peptide values during the course of the study. ITx: time of allogeneic islet transplantation. STZ: time of STZ injection for diabetes induction. Star: denotes time of cessation of immunosuppression. Triangle: First fasting blood glucose >160 mg/dL after allogeneic islet transplantation. C: Allogeneic islet

recipients show normal response to glucose challenge during the islet maintenance period, but display poor glucose tolerance upon withdrawal of immunosuppression.

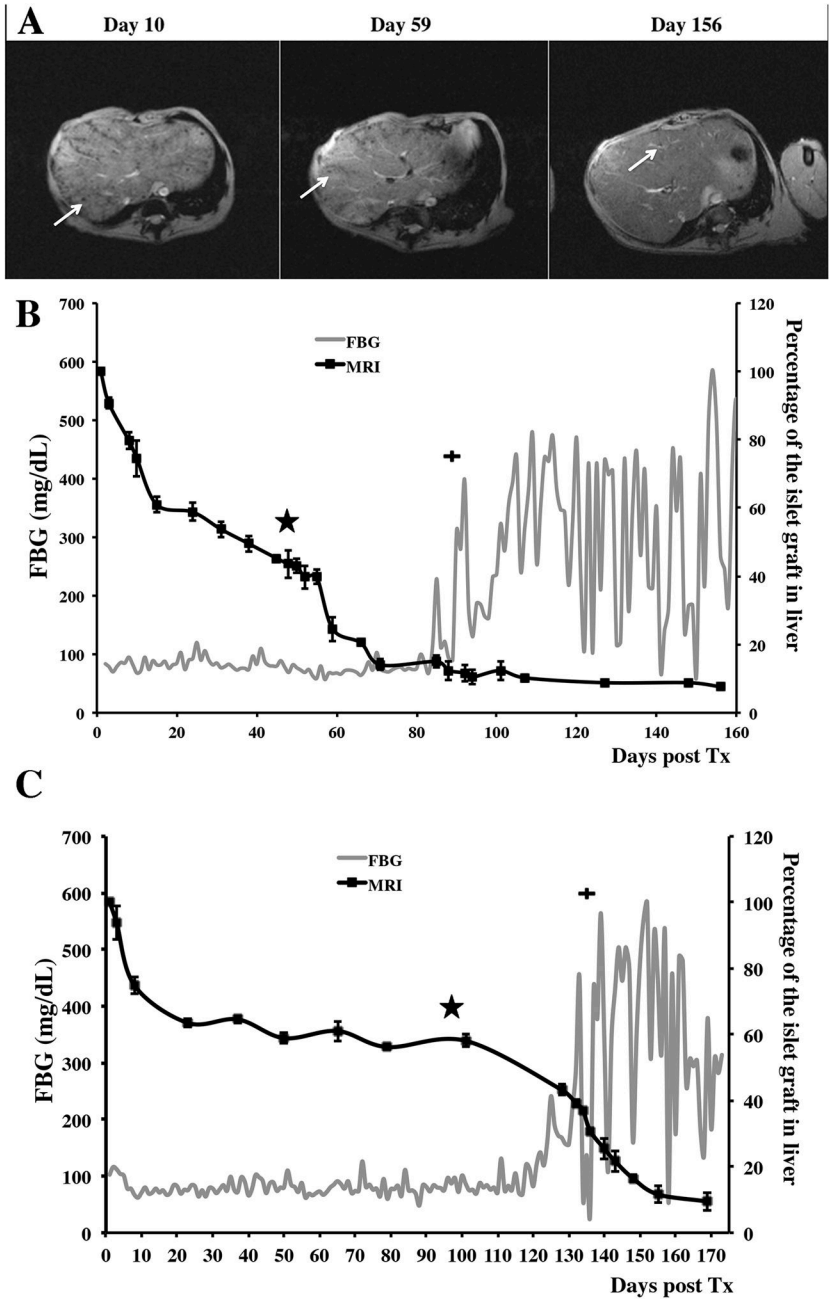

Figure 4.

Longitudinal MR imaging of allogeneic grafts. A: Representative T2* MR images of the allogeneic transplantation time course before withdrawal of immune suppression (day 2 shown), after withdrawal of immune suppression (day 59 shown), and the end stage (day 156 shown) (arrows – islets/islet clusters in the liver). B and C: Semiquantitative assessment of graft longevity by MRI (black line) demonstrates significant drop in graft volume followed by withdrawal of immunosuppression (star). FBG curve (grey line) during the post-immunosuppression withdrawal period (plus sign: Initiation of exogenous insulin therapy). (B – B183; C – B180)

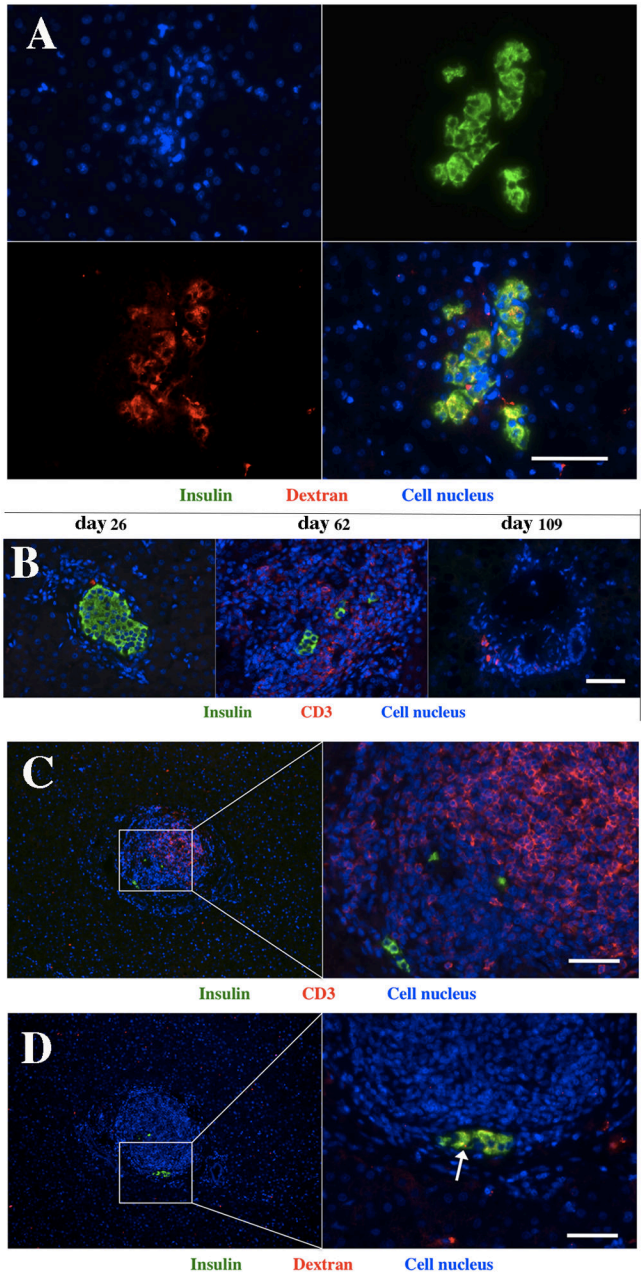

Figure 5.

Histological analysis of allogeneic islet grafts. A: Co-staining for insulin and dextran on the nanoparticles demonstrate abundance of the latter in islet cells in graft biopsy obtained before withdrawal of immunosuppression (green – insulin; red – dextran; blue – cell nucleus; magnification bar = 60 μm). B: Fluorescence microscopy demonstrates immunosuppression maintenance phase (day 26), and post-rejection period (day 62 and day 109) (green – insulin; red – CD3 T cells; blue – cell nucleus; magnification bar = 60 μm). C: Infiltrated islets showed the presence of residual insulin-positive cells (green – insulin; red – CD3 T cells; blue – cell nucleus; magnification bar = 50 μm). D: Section consecutive to the one shown in C demonstrates the presence of insulin-positive cells containing dextran-

coated iron oxide nanoparticles (white arrow); (green – insulin; red – dextran; blue – cell nucleus; magnification bar = 50 μm).